

Supplementary Information (SI) for Journal of Materials Chemistry C. This journal is © The Royal Society of Chemistry 2024

Supporting Information

On-demand optical printing of Ag-based neuromorphic devices for brain-inspired learning

Bharath Bannur^{a,*} & Sajan Daniel George^{a,b,*}

^aManipal Institute of Applied Physics, Manipal Academy of Higher Education, Manipal, 576104, India.

^bCenter for Applied Nanosciences (CANs), Manipal Academy of Higher Education, Manipal, 576104, India.

*Email: sajan.george@manipal.edu; bharath.b@manipal.edu



Figure S1. White rectangular pattern on a dark background prepared in PowerPoint for printing.

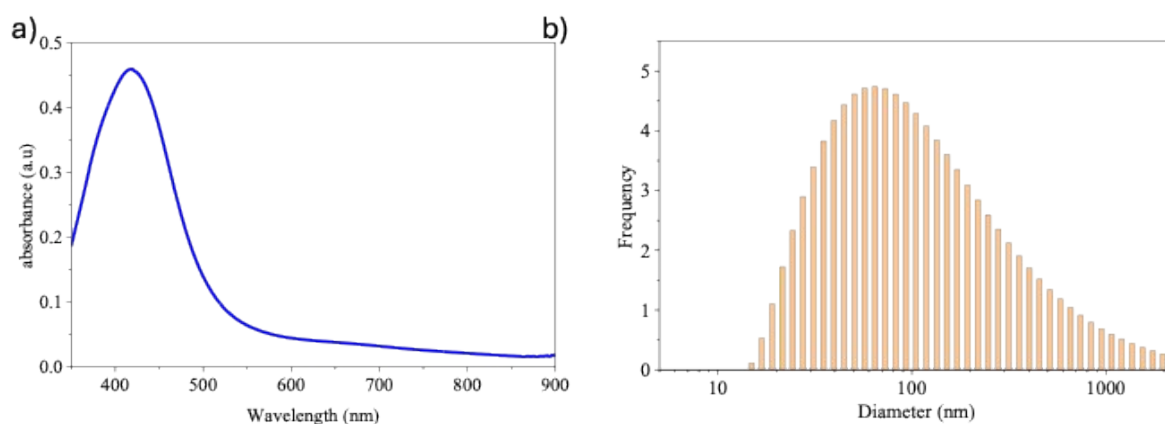


Figure S2. a) UV-Vis absorption spectrum of the prepared Ag colloidal solution. b) Particle size distribution of the Ag nanoparticles.

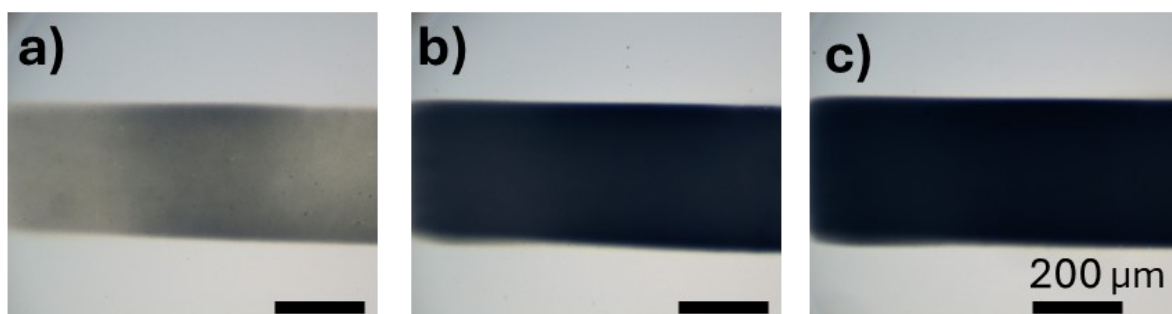


Figure S3. Optical images of prints obtained after 3, 6, and 9 minutes, showing reduced transmittance (increased opacity) with longer printing time, indicative of continuous film formation.

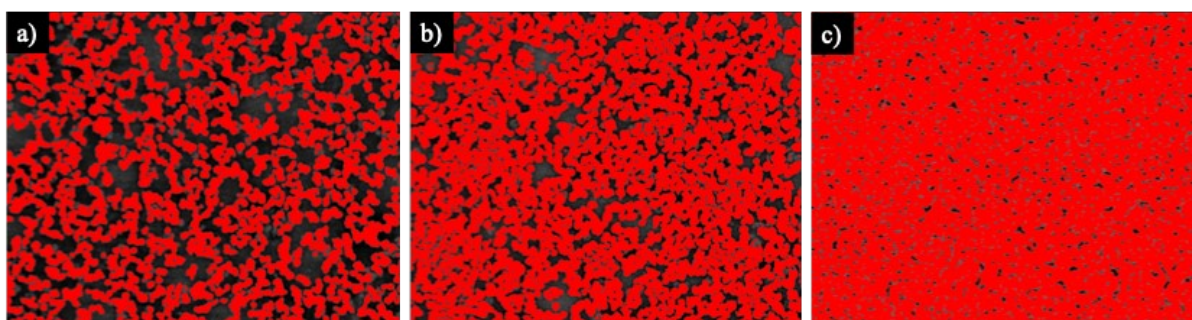


Figure S4. Fill factor analysis using FIJI (ImageJ) software for a) 3min b) 6min and 9) min printed film.

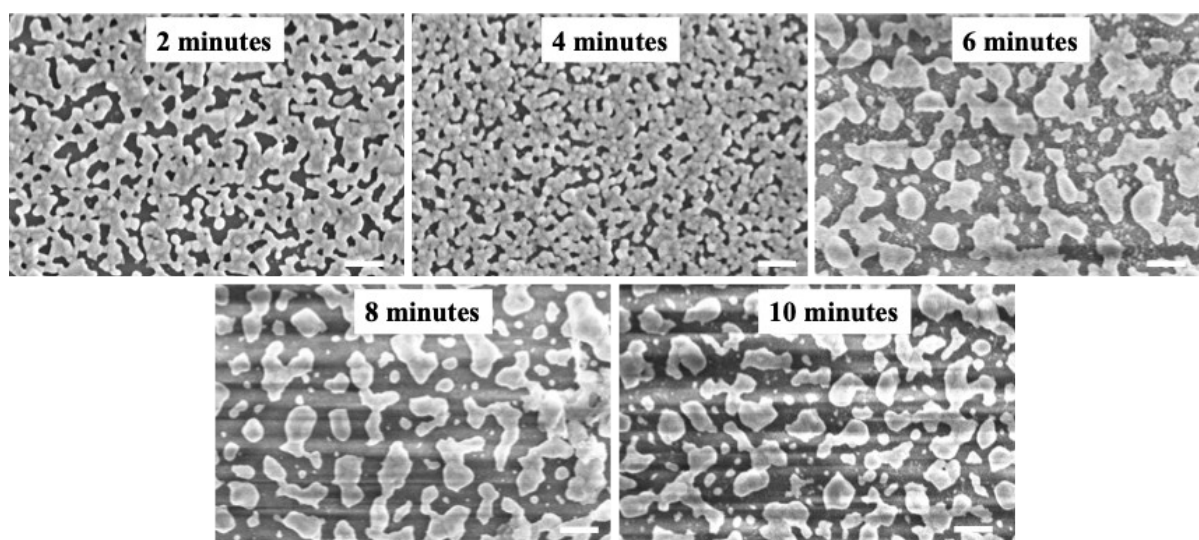


Figure S5. FESEM images of the Ag film annealed at 200 °C for varying time intervals. (scale bar: 500 nm)

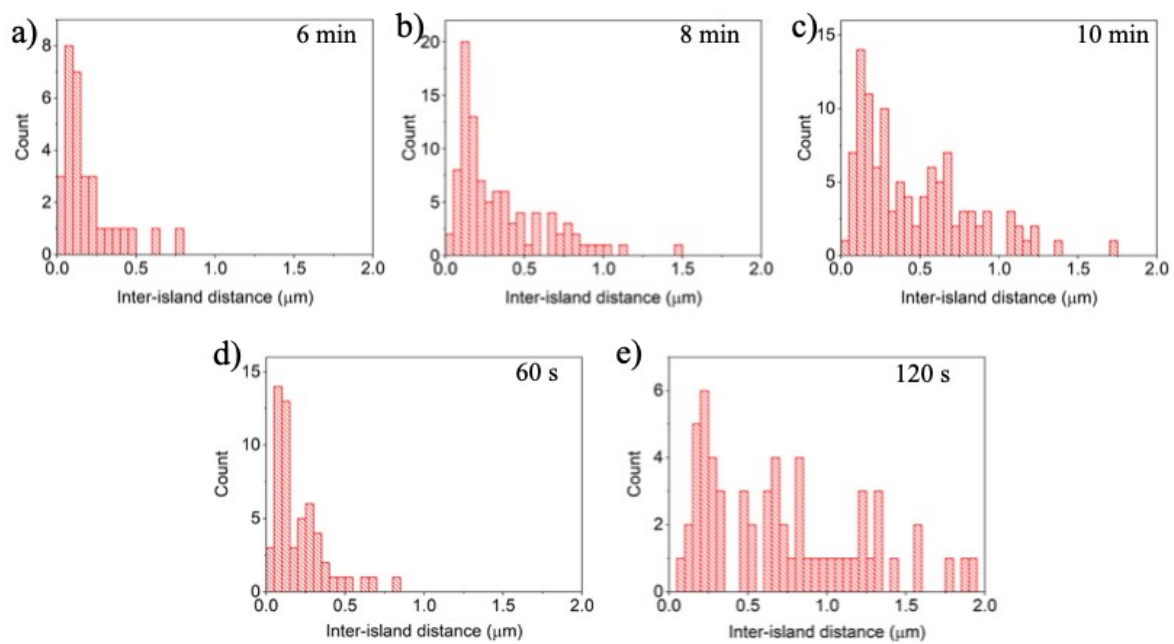
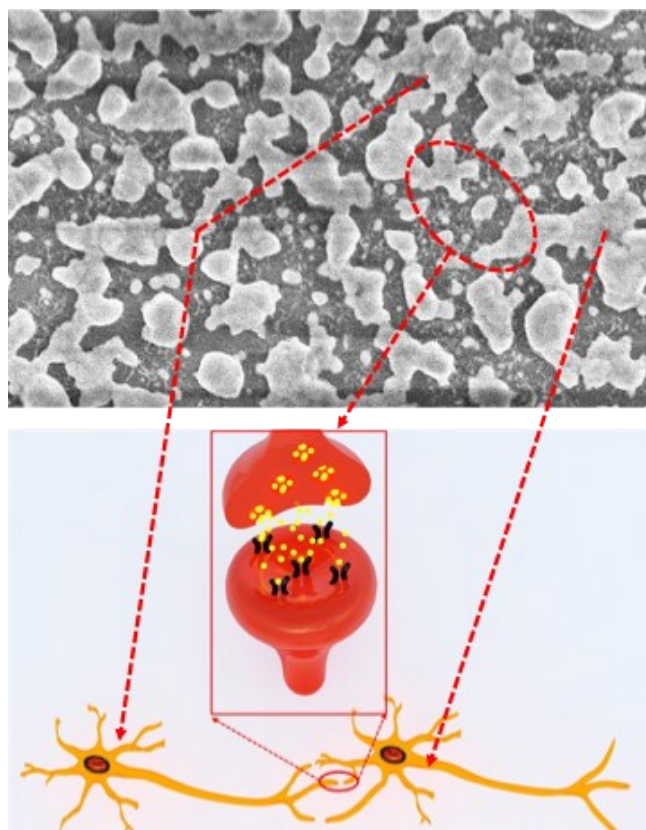


Figure S6. Statistical distributions of inter-island spacing for different annealing times at (a–c) 200 °C



and (d,e) 300 °C.

Figure S7. Illustration showing the resemblance between the Ag dewetted structure and a schematically represented bio-neural network.

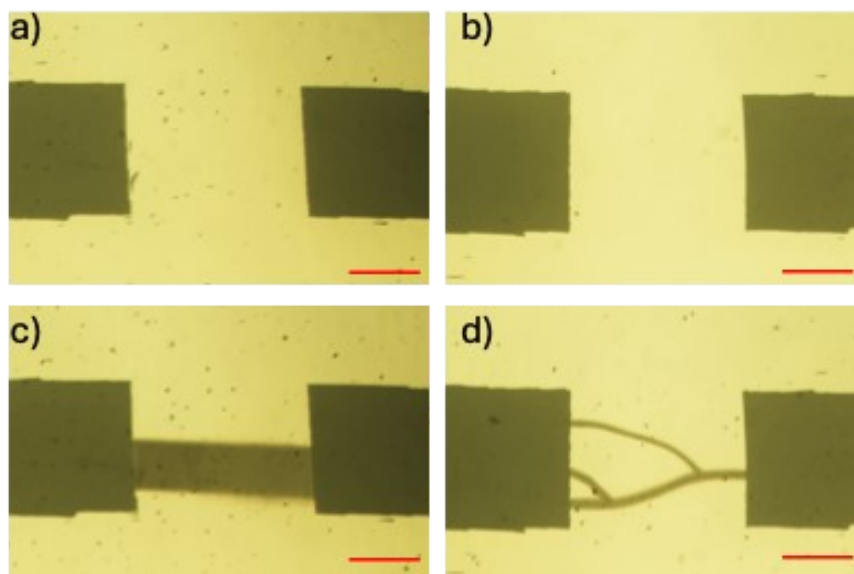


Figure S8. Ag particulate film printed across prefabricated Au electrodes, demonstrating on-demand printing capability. (Scale bar = 100 μm)

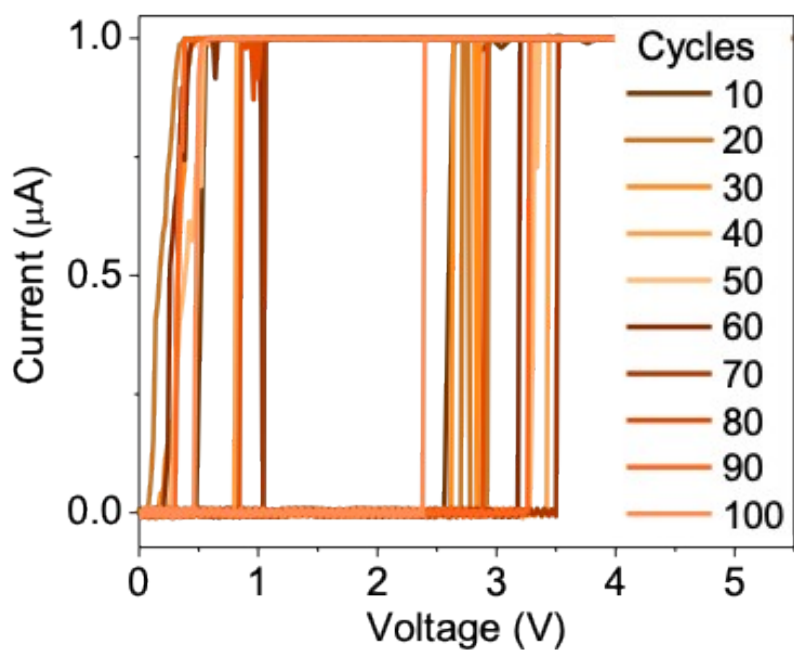


Figure S9. I–V characteristics of the device dewetted at 300 $^{\circ}\text{C}$ for 60 s. The device exhibited threshold switching at 3 ± 0.4 V.

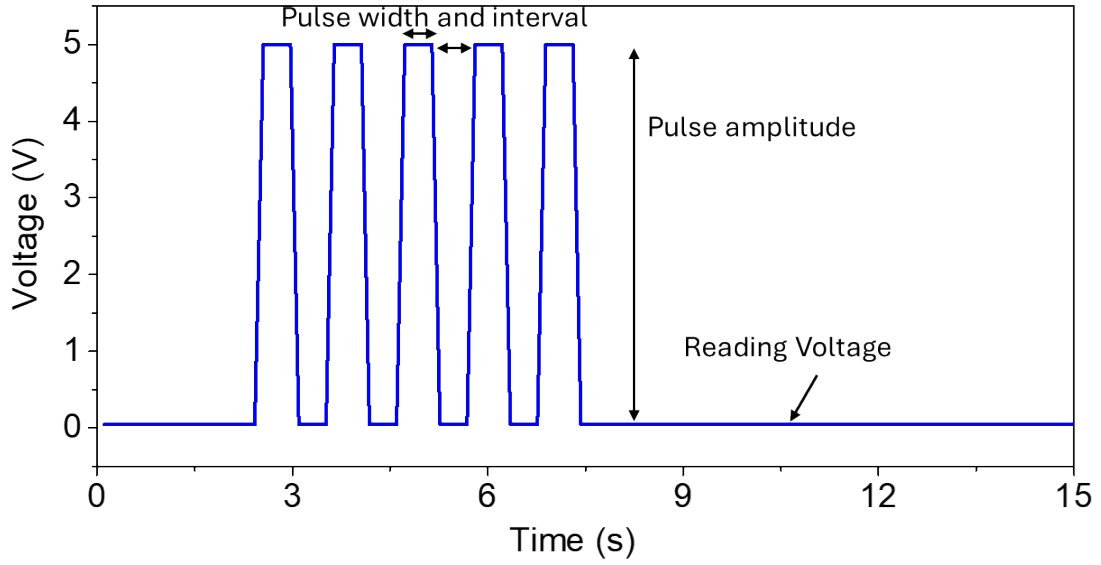


Figure S10. Pulse configuration used for emulating synaptic features.

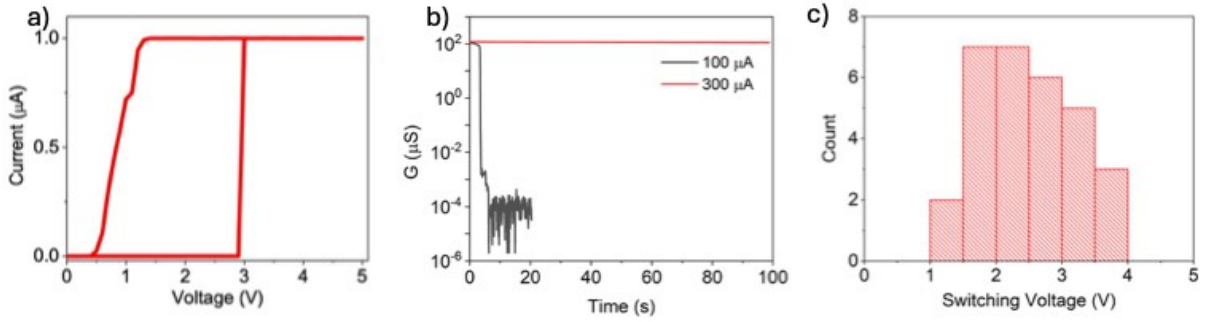


Figure S11. a) I-V characteristics of the device and b) STP and LTP (for 5 pulses of 5 V, 50 mV reading voltage) reproduced after 6 months showing the ambient stability and reproducibility. c) Switching voltage distribution of 15 devices studied for multiple cycles showing device to device variability.

Note S1:

Retention–reading voltage characteristics were fitted using an asymmetric Gaussian model as given below,

$$\text{Retention, } \tau(V_R) = A \cdot \exp\left(-\frac{(V_R - V_{opt})^2}{2\sigma(V_R)^2}\right), \sigma(V_R) = \begin{cases} \sigma_{L'} & V_R \leq V_{opt} \\ \sigma_{R'} & V_R > V_{opt} \end{cases} \text{-----(1)}$$

where A denotes the peak retention at the optimal reading voltage (V_{opt}). $\sigma(V_R)$ is the reading voltage-dependent width factor, where the parameters σ_L and σ_R represent the widths of the retention decay on the low- and high-voltage sides, respectively, capturing the asymmetric sensitivity of Ag filament stability to insufficient electric field (low V_R) and Joule-heating-driven dissolution (high V_R). A smaller σ value indicates higher sensitivity of the device to changes in the reading voltage. From the fitting, σ_L (0.064) was found to be smaller than σ_R (0.1), indicating that the retention is more sensitive on the low-voltage side.

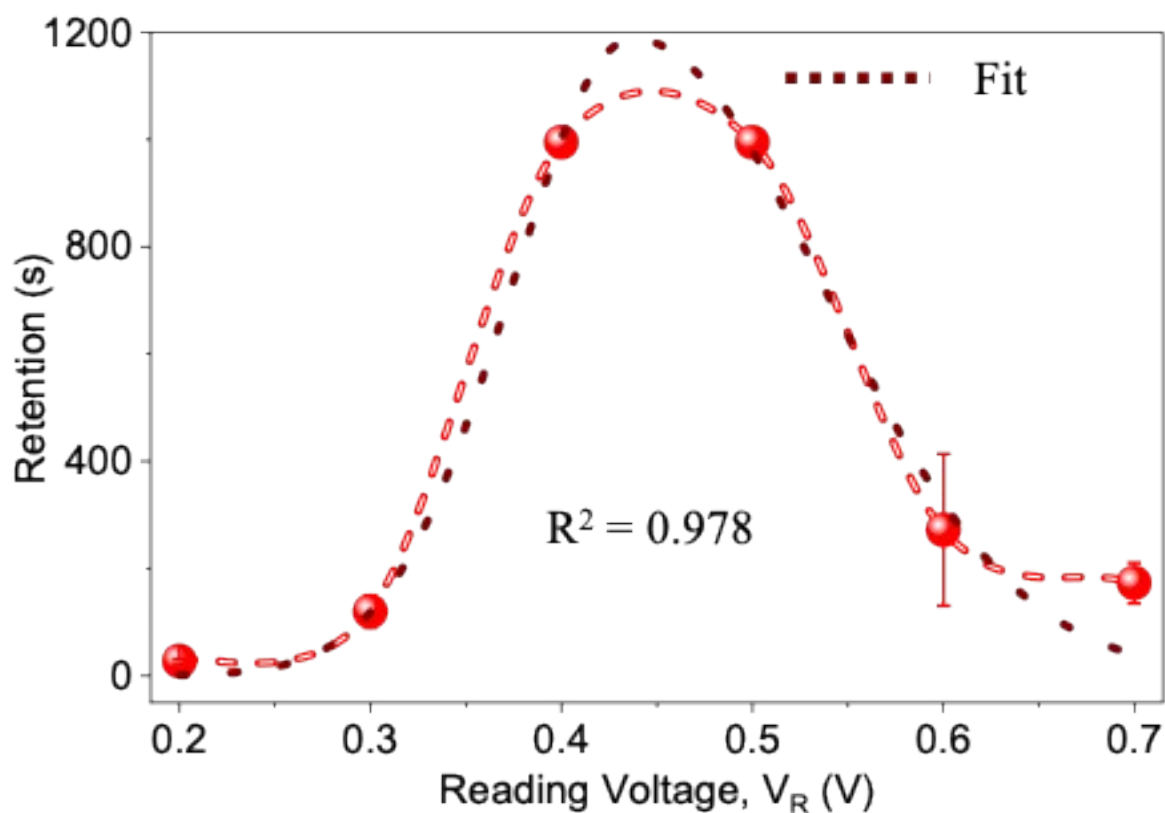


Figure S12. Modeling the inverted-U dependence using an asymmetric Gaussian function.

Table S1: Performance comparison of Ag artificial synaptic network (Ag-ASN)–based devices.

Process	Electrode geometry	Electrode gap (μm)	Switching voltage (V)	Remarks	Dewetting conditions	Ref.
Spin coating silver precursor → anneal→dewet	2-probe	10	1.89±0.55	Mechanistic insights into switching mechanism	270 °C for 30 s	1
	2-probe	10	1-4	Emulated STP, LTP associative learning		2
Vacuum deposition→anneal→dewet→vacuum deposition of Ag nanoparticles	2-probe	100	0.5	Flexible device, emulated STP, LTP, Associative learning	200 °C for 80 s	3
Vacuum deposition→anneal→dewet	IDT	10	0.43 ± 0.04	Emulated PPF, tip of the tongue experience	300 °C for 30 s	4
	IDT	10	0.42 ± 0.05	Excellent linearity, demonstrated arithmetic operations and number recognition		5
	IDT	10	0.45	Emulated STP, LTP, Supervision learning, nociception behaviour	300 °C for 40 s	6
	2-probe	-	0.6	Emulated STP, LTP 2 nd order associative learning	300 °C for 30 s	7
	2-probe	7	1.2	Emulated STP, LTP, Supervision learning, interest-based learning, associative learning		8
	Optical printing→anneal→dewet	2-probe	250	3.4 ± 0.4	Emulated STP, LTP, Yerkes-Dodson Law	200 °C for 6 min

STP – Short-term Plasticity, LTP – Long-term potentiation

References:

- 1 T. S. Rao, R. Gupta and G. U. Kulkarni, *Small*, 2025, **21**, 2502771.
- 2 T. S. Rao, I. Mondal, B. Bannur and G. U. Kulkarni, *Discov. Nano*, 2023, **18**, 124.
- 3 B. Yadav, I. Mondal, B. Bannur and G. U. Kulkarni, *Nanotechnology*, 2024, **35**, 015205.
- 4 M. Pal, N. S. Vidhyadhiraja and G. U. Kulkarni, *Adv. Funct. Mater.*, 2025, **35**, 2425635.
- 5 M. Pal, M. Kaur, B. Yadav, A. Bisht, V. N. S. and G. U. Kulkarni, *ACS Appl. Mater. Interfaces*, 2025, **17**, 5239–5253.
- 6 M. Pal, B. Yadav, I. Mondal, M. Kaur, N. S. Vidhyadhiraja and G. U. Kulkarni, *Nanoscale*, 2025, **17**, 19434–19446.
- 7 B. Bannur, B. Yadav and G. U. Kulkarni, *ACS Appl. Electron. Mater.*, 2022, **4**, 1552–1557.
- 8 B. Bannur and G. U. Kulkarni, *Mater. Horiz.*, 2020, **7**, 2970–2977.